

available at www.sciencedirect.comwww.elsevier.com/locate/brainres**BRAIN
RESEARCH**

Research Report

Protein expression and mRNA cellular distribution of the NKCC1 cotransporter in the dorsal root and trigeminal ganglia of the rat

Theodore J. Price^{a,b,*}, Kenneth M. Hargreaves^b, Fernando Cervero^a

^aMcGill University, Departments of Anesthesia and Dentistry and McGill Centre for Research on Pain, 3655 Prom Sir William Osler, Montreal, QC, Canada H3G 1Y6

^bThe University of Texas Health Science Center at San Antonio, Department of Endodontics and Pharmacology, 7703 Floyd Curl Dr., San Antonio, TX 78229, USA

ARTICLE INFO

Article history:

Accepted 5 July 2006

Available online 10 August 2006

Keywords:

Pain

Hyperalgesia

Chloride cotransporter

GABA

NKCC1

DRG

Trigeminal

Primary afferent neuron

Satellite glial cell

ABSTRACT

Primary afferent neurons maintain depolarizing responses to GABA into adulthood. The molecular basis for this GABAergic response appears to be the Na⁺K⁺2Cl⁻ cotransporter NKCC1 that contributes to the maintenance of a high intracellular chloride concentration. Recently, a role for NKCC1 has been proposed in nociceptive processing which makes it timely to gain a better understanding of the distribution of NKCC1 in sensory ganglia. Here, we describe that, in the rat, NKCC1 mRNA is predominately expressed by small and medium diameter dorsal root (DRG) and trigeminal (TG) ganglion neurons. The colocalization of NKCC1 mRNA with sensory neuron population markers was assessed. In the DRG, many NKCC1 mRNA-expressing neurons colocalized peripherin (57.0±2.5%), calcitonin-gene-related peptide (CGRP, 39.2±4.4%) or TRPV1 immunoreactivity (50.0±1.9%) whereas only 8.7±1.2% were co-labeled with a marker for large diameter afferents (N52). Similarly, in the TG, NKCC1 mRNA-expressing neurons frequently colocalized peripherin (50.0±3.0%), CGRP (35.4±2.6%) or TRPV1 immunoreactivity (44.7±1.2%) while 14.8±1.3% were co-labeled with the N52 antibody. NKCC1 mRNA was also detected in satellite glial (SGCs) in both the DRG and TG. Colocalization of NKCC1 protein with the SGC marker NG2 confirmed the phenotype of these NKCC1-expressing glial cells. In contrast to *in situ* hybridization experiments, we did not observe NKCC1 immunoreactivity in primary afferent somata. These findings suggest that NKCC1 is expressed in anatomically appropriate cells in order to modulate GABAergic responses in nociceptive neurons. Moreover, these results suggest the possibility of a functional role of NKCC1 in the glial cells closely apposed to primary sensory afferents.

© 2006 Elsevier B.V. All rights reserved.

* Corresponding author. Anaesthesia Research Unit, McGill University, McIntyre Medical Bldg. Room 1207, 3655 Promenade Sir William Osler, Montreal, Quebec, Canada H3G 1Y6. Fax: +1 514 398 8241.

E-mail address: theodore.price@mcgill.ca (T.J. Price).

Abbreviations:

CaMKII α , calcium-calmodulin-dependent kinase II α
 CGRP, calcitonin gene-related peptide
 DRG, dorsal root ganglion
 IHC, immunohistochemistry
 ISH, in situ hybridization
 KCC2, K, Cl cotransporter type 2
 N52, neurofilament 200 mouse monoclonal antibody
 NKCC1, Na, K, 2Cl transporter type 1
 NKCC2, Na, K, 2Cl transporter type 2
 NT, N-terminally directed rabbit polyclonal NKCC1 antibody
 SGC, satellite glial cell
 TEFS-2, C-terminally directed rabbit polyclonal NKCC1 antibody
 T4, mouse monoclonal antibody raised against a homologous region of NKCC1 and NKCC2
 TG, trigeminal ganglion
 TRPV1, transient receptor potential vanilloid type 1

1. Introduction

Intracellular chloride concentration in neurons is maintained by members of the Na⁺K⁺2Cl⁻ (NKCC) and K⁺Cl⁻ (KCC) families of cation–chloride cotransporters (for a review, see Payne et al., 2003). The NKCC proteins accumulate chloride intracellularly, whereas KCC cotransporters extrude chloride from the cell. The regulation of intracellular chloride concentration is important for a variety of physiological processes, and it is the primary mechanism that sets the reversal potential for chloride conductance through GABA_A receptors (GABA_AR) in neurons (Payne et al., 2003). Unlike most CNS neurons, dorsal root (DRG) and trigeminal (TG) ganglion neurons maintain depolarizing responses to GABA_AR agonists throughout postnatal development (Alvarez-Leefmans et al., 1988; Sung et al., 2000; Toyoda et al., 2005). The molecular basis for these depolarizing GABA_AR responses appears to be NKCC1 expression because depolarizing GABA_AR responses in DRG neurons are reduced in NKCC1^{-/-} mice (Sung et al., 2000).

Primary afferent depolarization (PAD) is known to underlie presynaptic inhibition in the spinal cord (for a review, see Rudomin and Schmidt, 1999; Schmidt, 1971). PAD decreases the magnitude of incoming action potentials leading to a reduction in the amount of transmitter released by primary afferent neurons. Moreover, PAD is mediated by GABA release from spinal interneurons as PAD is reduced by GABA_AR antagonists (Rudomin and Schmidt, 1999; Willis, 1999). Recently, it has been proposed that some enhanced pain states might involve enhancements of PAD such that, rather than inhibiting incoming action potentials, they induce a direct activation of spinal nociceptors causing both antidromic (also known as dorsal root reflexes (DRR; Willis, 1999) and orthodromic firing of these afferent fibers (Cervero

and Laird, 1996; Garcia-Nicas et al., 2006). This process requires increases in the depolarizing response to GABA_AR stimulation, and this has led to the proposal that NKCC1 is responsible for the increase in intracellular chloride that might mediate an enhanced PAD (Cervero et al., 2003; Price et al., 2005; Willis, 1999). In support of this hypothesis, it has been shown that NKCC1^{-/-} mice display reduced responses to noxious heat (Sung et al., 2000) as well as reduced touch-evoked pain (Laird et al., 2004). Furthermore, intrathecal delivery of the NKCC antagonist bumetanide inhibits nociceptive behavior in phase II of the formalin test (Granados-Soto et al., 2005). Finally, intracolonic capsaicin injection stimulates a rapid and transient increase in spinal phosphorylated NKCC1 and a longer lasting increase in trafficking of NKCC1 protein to the membrane (Galan and Cervero, 2005). Taken together, these findings indicate that NKCC1 might be an important player in inflammatory and tissue damage pain.

The current study was undertaken to gain a better understanding of the distribution of NKCC1 mRNA and protein in primary afferent neurons. Previous studies have indicated that NKCC protein can be detected in virtually all DRG neurons in the rat (Alvarez-Leefmans et al., 2001) and mouse (Sung et al., 2000). On the other hand, in situ hybridization studies have not clearly indicated that NKCC1 mRNA is expressed by all DRG (Kanaka et al., 2001) and TG (Toyoda et al., 2005) neurons. Moreover, the phenotype of these NKCC1 mRNA-expressing DRG and TG neurons has not been studied. Here, we have addressed the phenotypic distribution of NKCC1 mRNA and protein (using N- and C-terminally directed NKCC1 specific antibodies) in the DRG and TG of adult rats. A better understanding of the localization of NKCC1 can provide anatomical evidence to support current theories concerning PAD and its role in hyperalgesic states.

2. Results

2.1. Positive controls for NKCC1 in situ hybridization (ISH) and immunohistochemistry (IHC)

To assess that the NKCC1 riboprobe and antibodies labeled CNS regions in a manner consistent with previous reports, we assessed NKCC1 expression in the cerebellum and choroid plexus. NKCC1 mRNA-positive cells were seen in the granular layer of the cerebellum as well as in glia of the white matter tracts (Fig. 1A), consistent with previous reports (Kanaka et al., 2001; Mikawa et al., 2002). We examined the protein expression of NKCC1 in the cerebellum and choroid plexus using affinity-purified rabbit polyclonal antibodies directed against the N-terminus (NT; McDaniel et al., 2005; Wang et al., 2003) and C-terminus (TEFS-2; Del Castillo et al., 2005) of human NKCC1 (kindly provided by Dr. Christian Lytle, University of California at Riverside). Both the NT (Fig. 1B) and TEFS-2 (Fig. 1C) NKCC1 antibodies showed a similar pattern in the white matter and granular layer as observed for NKCC1 mRNA. Cells in the molecular layer were rarely labeled, and signal was not observed in Purkinje cells. KCC2 mRNA, on the other hand, was strongly expressed by Purkinje cells (Fig. 1F inset; Kanaka et al., 2001; Mikawa et al., 2002). Moreover, an intense NKCC1 mRNA (Fig. 1D) and immunoreactivity (NT antibody, Fig. 1E; TEFS-2 antibody, Fig. 1F) signal was observed in the choroid plexus (Kanaka et al., 2001; Plotkin et al., 1997).

2.2. NKCC1 protein and mRNA expression by Western blot and RT-PCR in the dorsal root, DRG, sciatic nerve and spinal dorsal horn

We first examined the distribution of NKCC protein and mRNA in the dorsal root, DRG, sciatic nerve and spinal dorsal horn by Western blot and PCR. NKCC protein was detected by the T4 monoclonal antibody (which recognizes both NKCC1 and NKCC2) as an ~160 kDa band by Western blot in all tissues examined (Fig. 2A). NKCC1 mRNA was also detected in these tissues by RT-PCR. Since the T4 monoclonal antibody also recognizes NKCC2 (Lytle et al., 1995), we examined NKCC2 mRNA expression in dorsal root, DRG, sciatic nerve and the spinal dorsal horn. We confirmed previous findings (Payne et al., 2003) that NKCC2 mRNA was not found in any of these tissues (Figs. 2B and 7D). However, NKCC2 mRNA was detected in the kidney (positive control tissue, Figs. 2B and 7E). These data confirm that NKCC2 is not present in the neural tissues examined in our experiments and, therefore, the bands recognized by the T4 antibody are likely to reflect NKCC1 or an NKCC1-like protein.

2.3. NKCC1 mRNA in the DRG, TG: colocalization with population markers and neuron size distribution

NKCC1 mRNA was found in a subpopulation of DRG ($52.6 \pm 2.8\%$) and TG ($50.1 \pm 2.5\%$) neurons. In addition to neurons, NKCC1 mRNA was detected in other cell types in both ganglia including satellite glial cells (SGCs, Figs. 2C and D). No signal

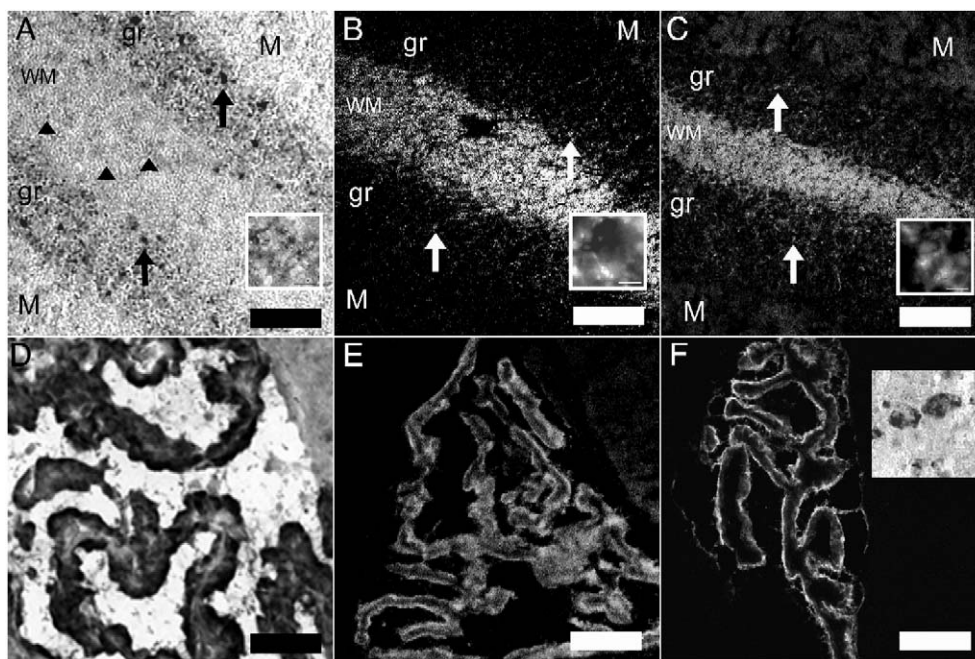


Fig. 1 – Positive controls for NKCC1 ISH and IHC: NKCC1 mRNA (A) and immunoreactivity with the NT (B) and TEFS-2 (C) antibodies in the cerebellum. WM=white matter, gr=granular layer, M=molecular layer. Upward arrows illustrate examples of NKCC1-positive cells in the granular layer. Arrowheads show examples of NKCC1 mRNA-positive glia in the white matter tract. Insets in each panel show 100× images of glia cells expressing NKCC1 mRNA or protein in WM tracts (scale bar=10 μm) NKCC1 mRNA (D) and immunoreactivity with the NT (E) and TEFS-2 (F) antibodies in choroid plexus. Inset in F shows KCC2 mRNA expression in cerebellar Purkinje cells. Scale bar=100 μm.

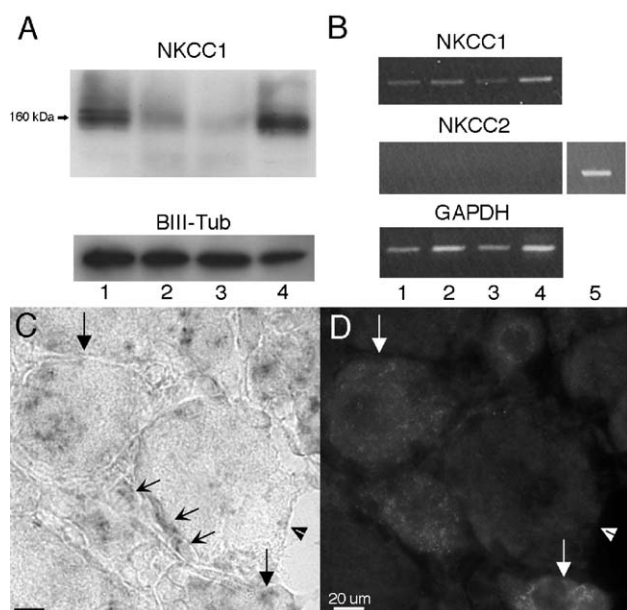


Fig. 2 – Assessment of NKCC1 protein and mRNA in dorsal root, DRG, sciatic nerve and spinal dorsal horn and NKCC1 mRNA expression in the DRG: (A) representative Western blots illustrating the presence of NKCC1 protein detected as a band at 160 kDa from dorsal root (1), DRG (2), sciatic nerve (3) and dorsal horn (4) protein homogenates (10 µg protein/lane). β-III tubulin was utilized as a loading control.

(B) Representative RT-PCR illustrating the presence of NKCC1 mRNA in the dorsal root (1), DRG (2), sciatic nerve (3) and dorsal horn (4) and the absence of NKCC2. Kidney (5) RNA was utilized as a positive control for NKCC2. GAPDH mRNA was used as a loading control. (C) High magnification (100×) image of NKCC1 mRNA in the DRG and the corresponding CGRP IHC image (D). Downward arrows: NKCC1 mRNA- and CGRP-expressing neurons. Arrowheads: large diameter NKCC1 mRNA- and CGRP-negative neuron. Concave diagonal arrows: NKCC1 mRNA-expressing glial cells in the DRG. Many of these cells appeared to be satellite glial cells (SGCs) based on their location ensheathing the soma of neurons.

was seen with a sense NKCC1 riboprobe (data not shown). We wanted to examine if NKCC1 mRNA is expressed by DRG and TG neurons that might be nociceptors. To test this hypothesis, we utilized a number of antibodies that identify subsets of sensory neurons with known properties. Peripherin is a neurofilament expressed by unmyelinated sensory neurons (Goldstein et al., 1991). In both the DRG (Figs. 3A, B) and TG (Figs. 4A, B) we observed an ~50% overlap between NKCC1 mRNA-positive neurons and peripherin immunoreactivity (Figs. 5A, B). On the other hand, we observed only a small degree of colocalization between NKCC1 mRNA-containing DRG (Figs. 3C, D) and TG (Figs. 4C, D) neurons and neurofilament 200 (N52)-immunoreactive cells (a marker for myelinated sensory neurons, ~10–20%, Figs. 5A, B). We also examined colocalization with calcitonin-gene-related peptide (CGRP) and transient receptor potential vanilloid type 1 (TRPV1). CGRP is a peptide neurotransmitter expressed by C- and A δ -fibers, many of which are nociceptors (Lawson

et al., 1996). In both the DRG (Figs. 3E, F) and TG (Figs. 4E, F), there was an ~50% degree of colocalization between CGRP-immunoreactive and NKCC1 mRNA-positive neurons (Figs. 5A, B). TRPV1, the capsaicin receptor, is expressed by a subpopulation of nociceptors (Caterina et al., 1997, 2000).

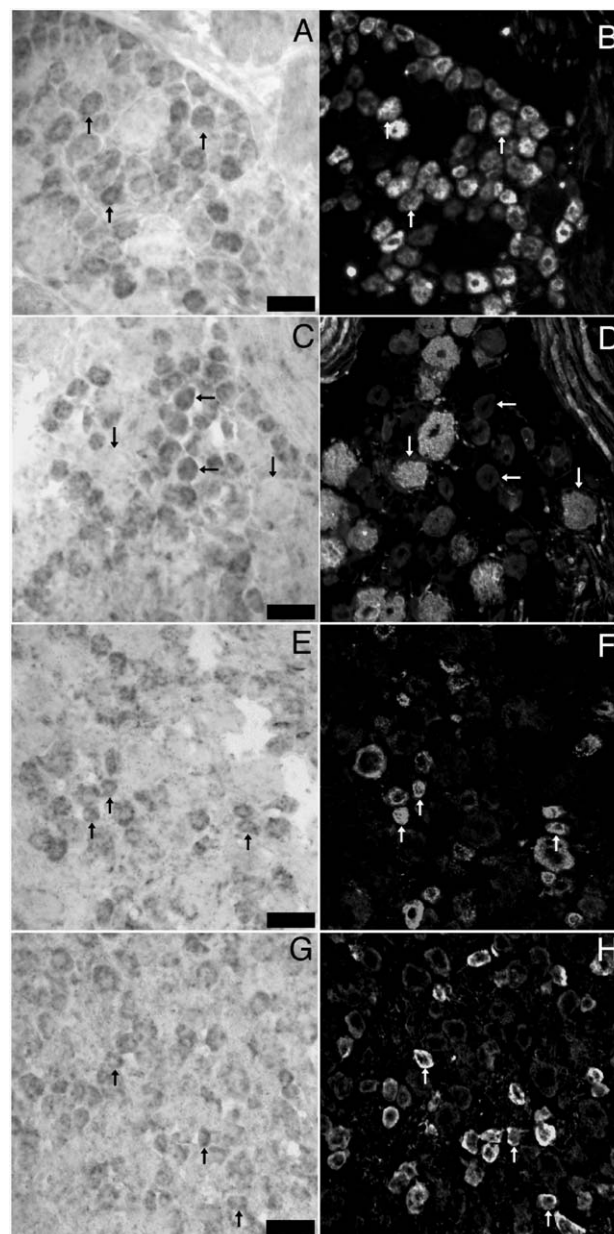


Fig. 3 – In situ hybridization for NKCC1 mRNA combined with immunohistochemistry for sensory neuron population markers in DRG: representative 40× photomicrographs of NKCC1 mRNA (A, C, E and G) combined with immunohistochemistry for peripherin (B), N52 (D), CGRP (F) and TRPV1 (H). Pairs of images are of the same field from double-labeled sections of lumbar DRGs. Upward arrows indicate examples of neurons, wherein colocalization of marker with NKCC1 mRNA was evident. Horizontal arrows in C and D illustrate NKCC1 mRNA-positive neurons that did not contain N52 immunoreactivity. Downward arrows show the converse. Scale bars = 100 µm.

Using a C-terminally directed TRPV1 antibody, we observed that there was 50–65% overlap (Figs. 5A, B) between NKCC1 and TRPV1 in both the DRG (Figs. 3G, H) and TG (Figs. 4G, H). Similar results were obtained with an N-terminally directed TRPV1 rabbit antibody (data not shown).

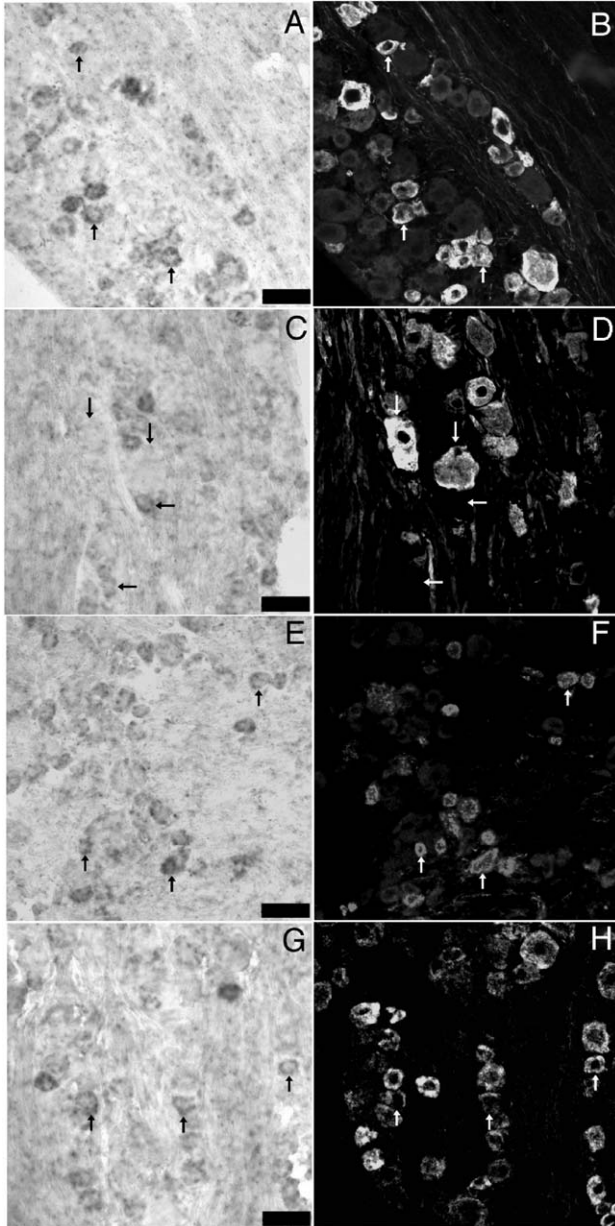


Fig. 4 – In situ hybridization for NKCC1 mRNA combined with immunohistochemistry for sensory neuron population markers in TG: representative 40× photomicrographs of NKCC1 mRNA (A, C, E and G) combined with immunohistochemistry for peripherin (B), N52 (D), CGRP (F) and TRPV1 (H). Pairs of images are of the same field from double-labeled sections of lumbar TGs. Upward arrows indicate examples of neurons, wherein colocalization of marker with NKCC1 mRNA was evident. Horizontal arrows in C and D illustrate NKCC1 mRNA-positive neurons that did not contain N52 immunoreactivity. Downward arrows show the converse. Scale bars = 100 μm.

We also constructed histograms of the diameters of neuronal profiles to gain a better understanding of the population of neurons in the DRG and TG that contain NKCC1 mRNA. NKCC1 mRNA signal was seen primarily in small to medium diameter DRG (Fig. 5C) and TG (Fig. 5D) neurons ranging from 20 to 30 μm. Comparison with TRPV1 and N52 diameter profile histograms demonstrated that NKCC1 mRNA-positive neurons have diameters similar to TRPV1-positive neurons, presumably nociceptors, whereas N52-positive profiles were larger in diameter, consistent with the myelination status of those neurons (Figs. 5C, D). The distributions of TRPV1 and N52 diameter profiles were consistent with previously published measurements (Guo et al., 1999; Hammond et al., 2004).

NKCC1 activity can be modulated through the phosphorylation of the transporter by a number of kinases. One such potential kinase is calcium/calmodulin-dependent kinase II α (CaMKIIα, Schomberg et al., 2001). Because CaMKIIα is expressed only by a subset of DRG neurons, many of which contain TRPV1, we sought to assess the colocalization of CaMKIIα with NKCC1. In the DRG, CaMKIIα and NKCC1 mRNA colocalized in ~55% of each of these populations (Fig. 6).

2.4. NKCC1 mRNA in the spinal cord

In the spinal cord, NKCC1 mRNA was detected in motor neurons and their surrounding cells of the ventral gray matter, as well as neurons of the deep lamina of the dorsal horn (Fig. 7A). NKCC1 mRNA was also found in the outer lamina of the spinal cord, however, fewer spinal neurons of the outer lamina were positive for NKCC1 mRNA as compared to the intense KCC2 mRNA signal seen throughout the dorsal horn (Fig. 7B). KCC2 mRNA was not observed in the DRG (Fig. 7C). NKCC2 (Fig. 7D) mRNA was not found in the DRG, whereas intense NKCC2 mRNA signal was observed in the medulla of the kidney (Fig. 7E, positive control for NKCC2 detection).

2.5. NKCC1 protein expression in the DRG and TG

We examined the protein expression of NKCC1 in the DRG and TG using affinity-purified rabbit polyclonal antibodies directed against the N-terminus (NT; McDaniel et al., 2005; Wang et al., 2003) and C-terminus (TEFS-2; Del Castillo et al., 2005) of human NKCC1. With both the NT and TEFS antibodies, we observed intense staining around the majority of neurons which appeared to be membrane localized NKCC1 in the DRG (Figs. 8 and 9) and TG (data not shown). However, this staining was particularly intense around large diameter N52 neurons (Figs. 8A–C and G–I) which was not consistent with the neuronal NKCC1 ISH data presented above. Interestingly, there was very little overlap between the N52 or TRPV1 immunoreactivity and the NKCC1-immunoreactive signal with either the NT or TEFS-2 antibody (Figs. 8C and I and 9C and F, respectively). This led us to investigate the possibility that the NKCC1 immunoreactivity observed surrounding neurons was contained within SGCs as indicated by the non-neuronal ISH localization. As shown in Fig. 2, within the DRG and TG, there were both neurons and resident glial cells, including SGCs, that expressed NKCC1 mRNA. The SGCs

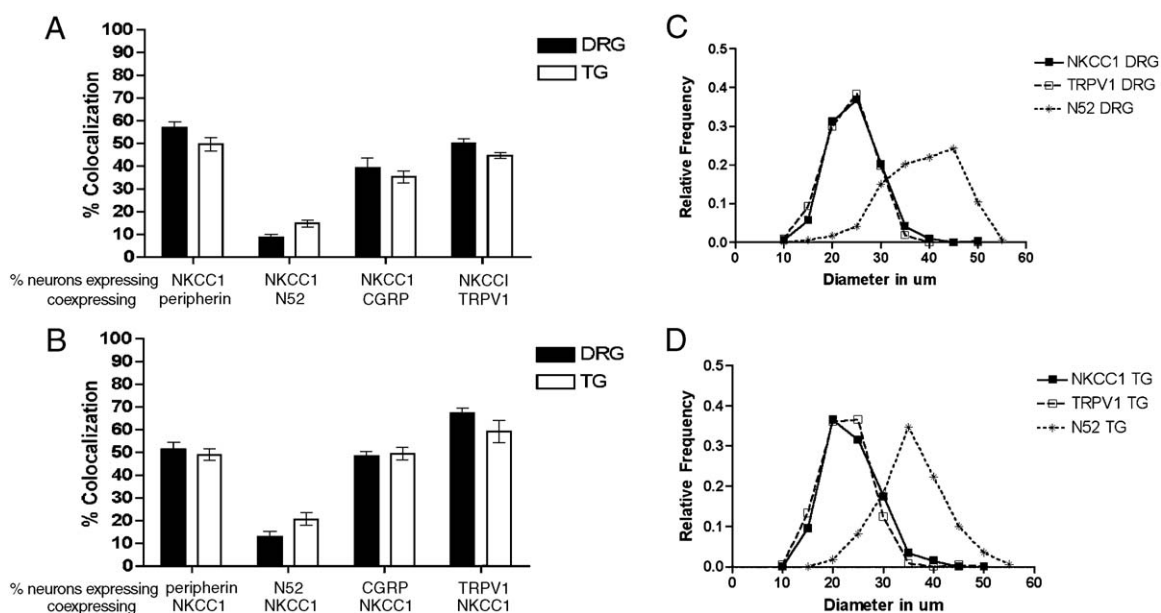


Fig. 5 – Percent colocalization of NKCC1 mRNA with sensory neuron population markers in DRG and TG and neuron size profiles: (A) the percentage of neurons positive for NKCC1 mRNA is shown as a function of neurons that also expressed peripherin, N52, CGRP or TRPV1 in both the DRG and TG ($n=3$ per condition). (B) The percentage of neurons that expressed peripherin, N52, CGRP or TRPV1 is shown as a function of the neurons that co-expressed NKCC1 mRNA in both the DRG and TG. NKCC1 mRNA-positive DRG (C) and TG (D) neurons neuron size relative frequencies are shown for 5 μm bins. The y axis shows the percentage of neurons that fall within a given 5 μm size range for the entire population. TRPV1-immunoreactive (small diameter marker) and N52-immunoreactive (large diameter marker) neuron size frequencies are also shown ($n=3$ per condition).

that encompass many DRG neurons are known to express the NG2 chondroitin-sulfate proteoglycan antigen (Rezajooi et al., 2004; Svenningsen et al., 2004); therefore, we examined colocalization of NKCC1 with NG2. There was a substantial colocalization of NKCC1 immunoreactivity, measured with both the NT and TEFS-2 antibodies, with NG2 in SGCs surrounding the majority of DRG neurons (Figs. 8F and L) and TG neurons (data not shown). Another non-neuronal cell type that contained NKCC1 immunoreactivity did not colocalize NG2 (Figs. 8E and F and K and L). We did not observe above background NKCC1 immunoreactivity with either NKCC1 antibody in DRG or TG neurons of any size.

3. Discussion

3.1. NKCC1 mRNA and protein expression in adult rat sensory ganglia

NKCC1 mRNA was detected in the DRG, dorsal root and sciatic nerve by RT-PCR, suggesting that NKCC1 mRNA is widely expressed in the PNS. NKCC1 mRNA was expressed by a subpopulation of DRG and TG neurons from adult rats, and these neurons were mostly small and medium in diameter. The colocalization of NKCC1 mRNA with peripherin and the subsequent lack of colocalization with N52 support this conclusion. We cannot exclude the possibility, however, that the ISH signal for NKCC1 was not sufficient to detect expression in large diameter neurons. Moreover,

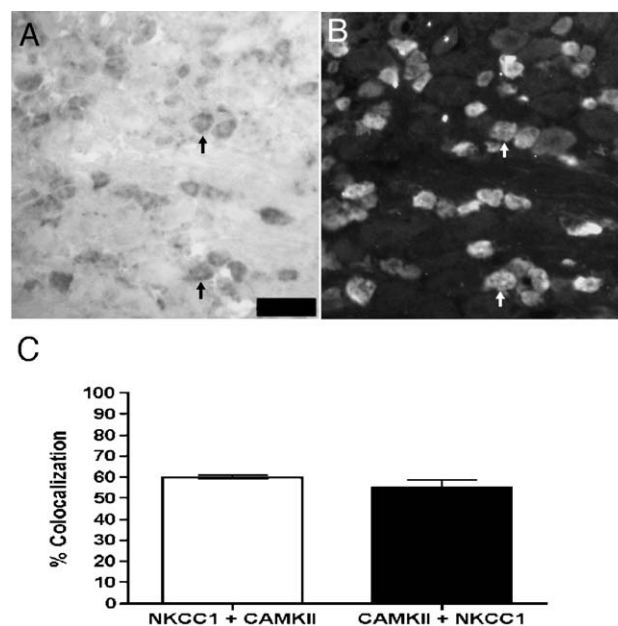


Fig. 6 – Colocalization of NKCC1 mRNA with CaMKII α protein in DRG: representative 40 \times photomicrographs of NKCC1 mRNA (A) with CaMKII α (B) immunoreactivity in the same DRG section. Upward arrows indicate examples of neurons co-expressing NKCC1 mRNA and CaMKII α protein. Scale bars = 100 μm . (C) Colocalization percentage for NKCC1 mRNA and CaMKII α protein in lumbar DRG sections ($n=3$ per condition).

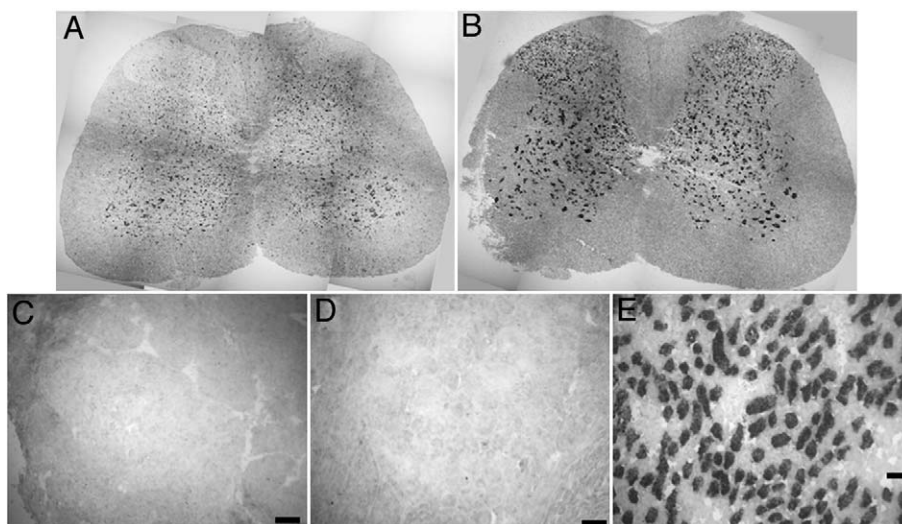


Fig. 7 – NKCC1 and KCC2 mRNA expression in spinal cord, lack of NKCC2 expression: images show in situ hybridization on whole lumbar spinal cord sections for NKCC1 mRNA (A) and KCC2 mRNA (B). Images are reconstructions from a series of 10× photomicrographs taken across the entire spinal cord section. Individual DRG photomicrographs showing a lack of KCC2 (C) and NKCC2 (D) mRNA expression in DRG, whereas NKCC2 mRNA was strongly expressed in the medulla of the kidney (E). Scale bars = 100 μm.

colocalization of NKCC1 mRNA with both CGRP and TRPV1 supports the hypothesis that NKCC1 plays a role in maintaining high intracellular chloride levels in peptidergic and nociceptive neurons, respectively. In the rat, expression of NKCC1 mRNA has been previously demonstrated in the DRG (Kanaka et al., 2001) and TG (Toyoda et al., 2005), although the precise population of NKCC1-expressing neurons was not identified. These studies indicated that many DRG and TG neurons express NKCC1 mRNA; however, our results indicate that NKCC1 mRNA expression is restricted to small and medium diameter sensory neurons. NKCC1 mRNA was also evident in small, round cells, whose morphology and localization within the ganglion are consistent with that of fibroblasts and/or Schwann cells as well as SGCs surrounding DRG and TG neurons which suggests a more widespread role for NKCC1 within these ganglia.

NKCC protein was detected with the T4 monoclonal antibody by Western blot in the DRG, dorsal root, sciatic nerve and dorsal horn. Since NKCC2 mRNA expression was completely absent from each of these tissues, it is likely that the molecular species identified by the T4 antibody is either NKCC1 or an NKCC1-like protein of very similar size. Previous studies with the T4 monoclonal antibody have indicated that NKCC protein localizes to the majority, if not all, of rat DRG neurons (Alvarez-Leefmans et al., 2001) and NKCC1 protein is likewise localized to the majority of mouse DRG neurons (Sung et al., 2000). These findings are not congruent with the data presented here. Hence, we assessed NKCC1 immunoreactivity in both the DRG and TG using rabbit polyclonal, affinity-purified N (NT, characterized in McDaniel et al., 2005; Wang et al., 2003)- and C (TEFS-2, characterized in Del Castillo et al., 2005)-terminally directed NKCC1 polyclonal antibodies. A labeling pattern that appeared to be either neuronal membrane localized NKCC1 immunoreactivity or SGC NKCC1 immunoreactivity was observed with both

NKCC1 antibodies. Because we observed little colocalization with either a cytoskeletal protein (neurofilament 200, N52) or an integral membrane protein (TRPV1), we investigated the possibility that NKCC1 immunoreactivity colocalized with NG2 chondroitin-sulfate proteoglycan antigen, a marker for SGCs of the PNS (Rezajooi et al., 2004; Svenningsen et al., 2004). The high degree of colocalization between NKCC1 (with both antibodies) and NG2, coupled with the lack of colocalization with N52 or TRPV1, strongly suggests that the previously observed “membrane” NKCC1 immunoreactivity in large DRG neurons does not represent neuronal NKCC1, but, rather, NKCC1 localized to SGCs. The physiological relevance of NKCC1 in SGCs is not known, but it is tempting to speculate that it might play a role in potassium buffering especially around large diameter neurons which have high firing rates (as proposed in Hanani, 2005). NKCC1 immunoreactivity was also evident in cells of both ganglia that were neither neurons nor SGCs. It is likely that these cells were either Schwann cells or fibroblasts based on their morphology and location within the ganglia; however, we did not pursue their phenotype further with immunohistochemical markers as these studies were beyond the scope of the present investigation.

Unexpectedly, we did not observe NKCC1 immunoreactivity in DRG or TG neurons of any size, even though NKCC1 mRNA was clearly expressed by a subpopulation of DRG and TG neurons. The reasons for this are unclear. One hypothesis is that NKCC1 protein is rapidly trafficked to central and peripheral terminals and is therefore at very low concentrations within the soma itself. If this were the case, it is reasonable to expect that NKCC1 immunoreactivity would be observed in cells that do not send projections outside the ganglion (like SGCs) whereas the amount of protein would be below detection limits within the soma of DRG or TG neurons, as we observed. We favor this hypothesis because

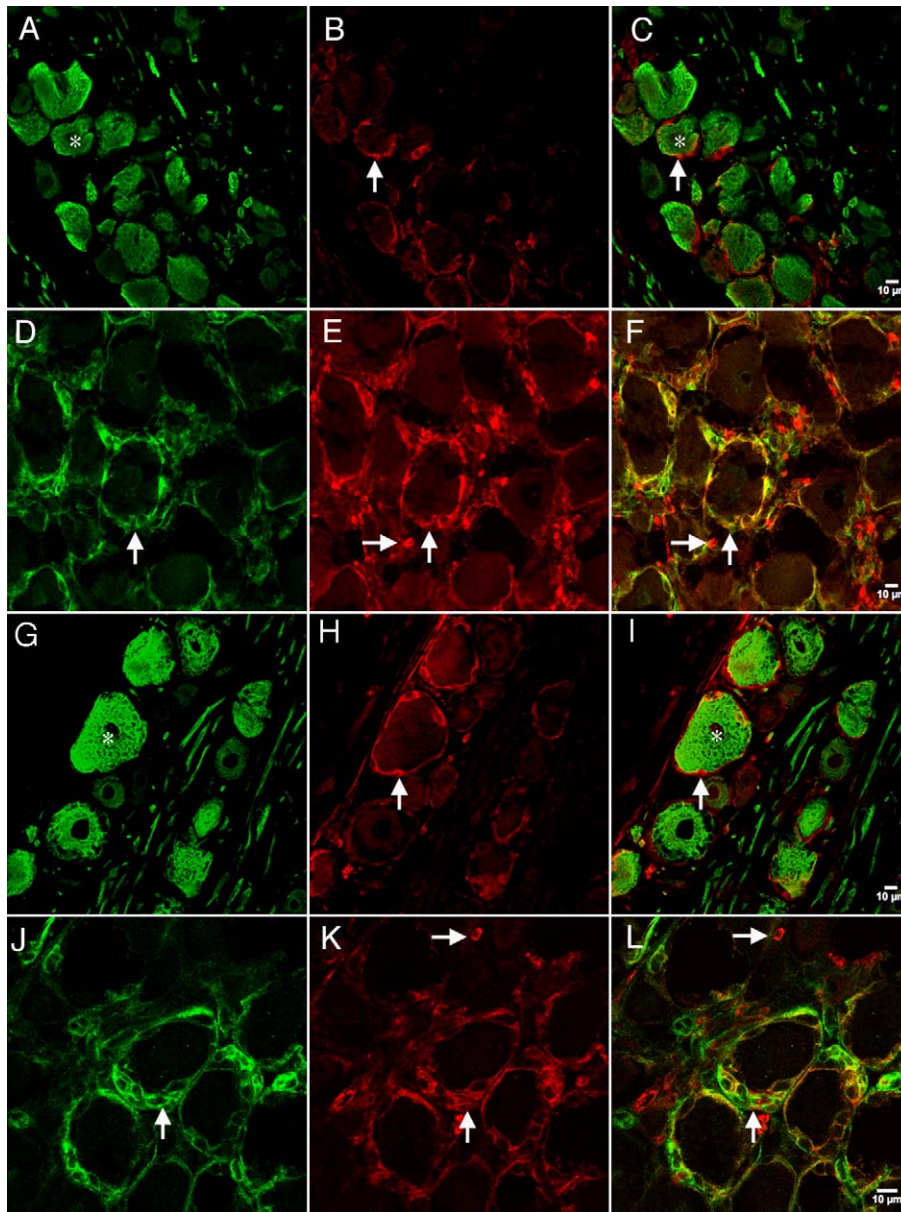


Fig. 8 – Confocal images of NKCC1 immunoreactivity with N52 or NG2 in the DRG: representative confocal photomicrographs of NKCC1 (NT) immunoreactivity utilizing the NT antibody (B and E) with N52 (A) or NG2 (D). NKCC1 (TEFS-2) immunoreactivity utilizing the TEFS-2 antibody (H and K) with N52 (G) or NG2 (J). Respective merged images are shown in panels C, F, I and L. Vertical arrows illustrate NKCC1 (NT)-immunoreactive SGCs surrounding neurons in B and C and E and F or NKCC1 (TEFS-2)-immunoreactive SGCs surrounding neurons in H and I and K and L. Vertical arrows in D and J illustrate NG2 immunoreactivity in these SGCs. Horizontal arrows in E and F and K and L demonstrate NKCC1 (NT)-immunoreactive non-neuronal cells that do not express NG2. Stars in A and C and G and I illustrate N52-immunoreactive neurons that are surrounded by NKCC1 (NT or TEFS-2, respectively)-immunoreactive cells.

both antibodies (which are directed against non-overlapping epitopes) showed identical staining patterns in the DRG, TG, cerebellum and choroids plexus and were congruent with NKCC1 mRNA signals in all these areas with the exception of DRG and TG neurons. Moreover, in further support of this notion, NKCC1 trafficking is known to play an important role in NKCC1 function and has been shown to occur in the spinal dorsal horn (Galan and Cervero, 2005) and dorsal rhizotomy reduces dorsal horn NKCC1 protein levels (Donna Hammond, personal communication). Such a discord between mRNA

and protein detection is not without precedent in sensory afferents. Peripherin mRNA is expressed by all DRG neurons, while peripherin immunoreactivity is only detected in the unmyelinated subset (Goldstein et al., 1991, 1996; Parysek et al., 1988). Moreover, the glycine receptor β subunit mRNA is expressed by DRG neurons but protein is not detectable through immunohistochemistry (Coggeshall and Carlton, 1997). We cannot, however, rule out the possibility that other factors contribute to this difference between the ISH and IHC data.

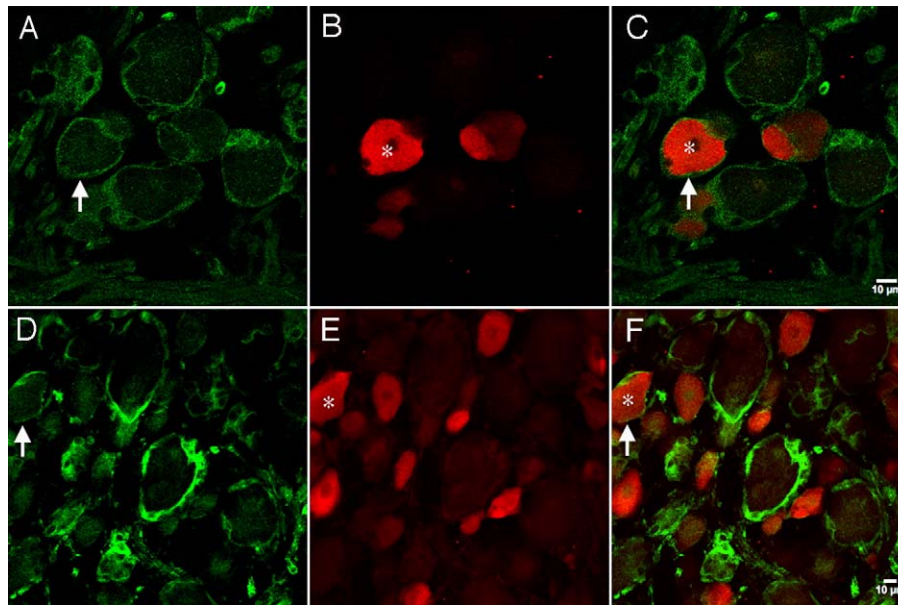


Fig. 9 – Confocal images of NKCC1 immunoreactivity with TRPV1: representative confocal photomicrographs of NKCC1, NT (A) or TEFS-2 (D), immunoreactivity with TRPV1 (B and E). Respective merged images are shown in panels C and F. Vertical arrows illustrate NKCC1 (NT (A and C) or TEFS-2 (D and F))-immunoreactive SGCs surrounding neurons. Stars in B and C and E and F illustrate TRPV1-immunoreactive neurons that are surrounded by NKCC1-immunoreactive SGCs.

3.2. Implications for chloride accumulation in sensory neurons

The observation that all adult rat DRG and TG neurons might not express NKCC1 mRNA requires alternative interpretations to explain the depolarizing actions of GABA in these cells. DRG neurons, of a variety of diameters, from NKCC1^{-/-} mice display altered GABA_AR-evoked currents indicating that NKCC1 is necessary for GABA-induced depolarization in these neurons (Sung et al., 2000). Olfactory receptor neurons (ORNs), like sensory neurons, express a depolarizing chloride current that is thought to be mediated by NKCC1-dependent chloride accumulation (Kaneko et al., 2004; Reisert et al., 2005). On the other hand, recordings made from ORNs in situ indicate that depolarizing chloride currents are largely intact in tissue from NKCC1^{-/-} mice (Nickell et al., 2005). While it is difficult to extrapolate findings from ORNs to DRG neurons, these discrepancies indicate that the role of NKCC1 in depolarizing chloride currents might be different in isolated or cultured neurons than in vivo or in situ. Since all primary afferents are known to depolarize in response to GABA (for a review, see Rudomin and Schmidt, 1999) and there seems to be a lack of NKCC1 mRNA in a subpopulation of these afferents, it appears that other mechanisms of depolarizing GABA_AR responses should be considered for large primary afferent neurons. Importantly, intracellular chloride concentrations have never been directly assessed in central terminals of primary afferents. Such a study could shed considerable light on this issue.

We found, in agreement with others, that NKCC2 (Payne et al., 2003) and KCC2 (Kanaka et al., 2001) transcripts were not expressed in the DRG. It has been shown that neurons of the premature lateral superior olive, even in the absence of KCC2

and NKCC1, can be depolarized by GABA (Balakrishnan et al., 2003). Moreover, GABAergic axo-axonic synapses onto adult cortical pyramidal neurons are capable of eliciting excitatory GABA_A-R currents (Szabadics et al., 2006). This effect was attributed to a lack of axonal KCC2 in these neurons, leading to a high intracellular chloride concentration (Szabadics et al., 2006). Cortical pyramidal neurons rarely respond to bumetanide (Zhu et al., 2005) and, in the absence of KCC2, do not respond to changes in extracellular potassium concentrations with concomitant alterations in intracellular chloride levels (DeFazio et al., 2000). This suggests that alternative chloride accumulation mechanisms must be at work in these neurons. Since sensory neurons do not express KCC2 and only a subpopulation appears to express NKCC1 mRNA, this also suggests that other chloride accumulation mechanisms should be considered for primary afferents. The T4 monoclonal antibody for NKCC protein appears to label all DRG neurons (Alvarez-Leefmans et al., 2001). However, it is possible that the T4 antibody recognizes another epitope that could participate in accumulating chloride in DRG neurons. It should also be noted that alternative ionic mechanisms could also be responsible for GABA_AR-dependent depolarizing currents. Bicarbonate reversal potentials are maintained at a more positive level with respect to the resting potential than chloride, and, in the presence of a collapse of the chloride gradient, bicarbonate outflow can lead to GABA_AR-dependent depolarization (Kaila et al., 1989; Staley et al., 1995). Moreover, sustained network activity, as might be expected in the dorsal horn of the spinal cord, can lead to GABA_AR-mediated, bicarbonate-dependent, extracellular potassium accumulation, causing long lasting depolarizing responses (Kaila et al., 1997; Rivera et al., 2005). Original theories concerning the ionic basis of PAD focused on GABA_ARs and extracellular potassium

dependency, with the potassium hypothesis being largely dismissed due to pharmacological findings indicating that PAD was GABA_AR-dependent (for a review, see Rudomin and Schmidt, 1999). Recent work has shown that potassium transients producing depolarization are GABA_AR-mediated and involve bicarbonate efflux (Kaila et al., 1997; Rivera et al., 2005) which implies that the mechanism of PAD generation might require alternative explanations, especially in the primary afferents that apparently lack NKCC1 mRNA.

3.3. Implications for nociception

The hypothesis that allodynia involves increases in PAD leading to the production of DRRs and a direct activation of spinal nociceptive neurons by activity in low threshold afferents (Cervero and Laird, 1996; Garcia-Nicas et al., 2006) predicts that NKCC1 would be a molecular target for the alterations in intracellular chloride that are required to achieve GABAergic DRRs (Cervero et al., 2003; Price et al., 2005; Willis, 1999). Consistent with this hypothesis, intracolonial capsaicin injection stimulates a rapid and transient increase in spinal phosphorylated NKCC1 and a longer lasting increase in trafficking of NKCC1 protein to the membrane (Galan and Cervero, 2005). However, it remains unclear if these molecular events occur only in primary afferent nociceptors or in other spinal neurons or glia. The finding that NKCC1 mRNA is predominantly localized to small and medium diameter DRG neurons, many of which are nociceptors, is consistent with the hypothesis that NKCC1 mediates DRRs in these neurons. Moreover, we observed little NKCC1 mRNA in the spinal dorsal horn, lending further support to this interpretation. While it is clear that NKCC1 must play a role in touch-evoked nociception since NKCC1^{-/-} mice have deficits in allodynia (Laird et al., 2004), the cellular mechanisms of this observation remain uncertain.

3.4. Conclusions

NKCC1 mRNA is expressed by a subpopulation of DRG and TG neurons, most of which are small and medium diameter and many of which are nociceptors because they also express TRPV1. NKCC1 mRNA and protein were also found in SGCs (confirmed by NG2 immunoreactivity) within the DRG and TG. These results indicate that PAD in the spinal cord may not be explained simply through GABA_AR-dependent depolarization mediated by chloride accumulation through NKCC1 and that other mechanisms must be taken into account. Moreover, the data presented here suggest that NKCC1 is likely to play a widespread role in sensory ganglia, especially with respect to its localization in SGCs.

4. Experimental procedures

4.1. Animals and tissue preparation

Adult male Sprague–Dawley rats (Harlan, Indianapolis, IN) weighing 175–225 g were used in this study. All procedures were approved by the Institutional Animal Care and Use Committees of McGill University and The University of Texas

Health Science Center at San Antonio and were conducted in accordance with policies for the ethical treatment of animals established by the National Institutes of Health. Rats were euthanized by decapitation, under halothane anesthesia, and their TGs, L4–6 DRGs, sciatic nerves, dorsal roots and spinal cords were quickly removed (~4 min) and fresh frozen on dry ice in OCT compound (Sakura, Torrance, CA) for immunohistochemistry (IHC) and/or in situ hybridization (ISH) or in liquid nitrogen for protein and PCR analysis. Tissue sections were cut (20 μm) on a Leica CM1800 cryostat (Bannockburn, IL), thaw-mounted (10 min at room temperature) onto Superfrost Plus glass slides (VWR, West Chester, PA) and stored at –80 °C until use. For each experimental condition, 2 TG, 3 DRG or 2 spinal cord sections were randomly chosen from each of three animals, and all ISH and IHC experiments were performed concurrently. RNA and proteins were isolated from 3 animals each for Western blotting and RT-PCR.

4.2. Western blotting

Frozen tissues were homogenized in standard RIPA buffer (Tris–HCl 50 mM, 1% Triton X-100, NaCl 150 mM and EDTA 1 mM, pH 7.4) with a motorized dounce homogenizer, sonicated for 15 min at 4 °C and cleared of cellular debris and nuclei by centrifugation at 13,000 RCF for 5 min at 4 °C. Ten micrograms of protein per well was loaded and run by standard SDS-PAGE. Proteins were transferred to Immobilon-P membranes (Millipore, Nepean, ON, Canada) and then blocked with 5% dry milk for 3 h at room temperature. NKCC antibody (T4 monoclonal antibody which recognizes both NKCC1 and NKCC2 (Lytle et al., 1995), Iowa Hybridoma Bank) was incubated overnight at 1:1000 dilution and detected the following day with anti-mouse immunoglobulins conjugated to horseradish peroxidase (Dako, Ottawa, Canada). Signal was detected by ECL-plus (Amersham/GE Healthcare) on chemiluminescent films (Kodak). Blots were then stripped using Restore reagent (Pierce, Rockford, IL) and reblotted with an anti-β-III tubulin antibody (1:1000, Promega, Madison, WI) as a loading control.

4.3. RT-PCR

Total RNA was isolated from frozen tissues using total RNA kits (Ambion, Austin, TX), and DNA was removed using DNA-free (Ambion). First strand cDNA synthesis was carried out using 1 μg RNA as a template using iScript cDNA synthesis kits (Biorad, Hercules, CA). PCR was then done using 50 ng cDNA with iTAQ DNA polymerase kits (Biorad) for 30 cycles with an annealing temperature of 55 °C on an MJ mini-thermal cycler (Biorad). Primers for NKCC1 were: fwd, 5' tgt tgg att cgc aga gac tg 3' and rev, 5' gtt cct ttg ggt atg gct ga 3' and NKCC2 were: fwd, 5' caa gac ctg ctc tcc tgg ac 3' and rev, 5' agc cag tct ctc ctg ttc ca 3'. Rat GAPDH primers (Biorad) were used as a positive control.

4.4. In situ hybridization (ISH)

All chemicals were from Sigma (St. Louis, MO) unless otherwise stated. cDNA fragments were amplified from reverse transcribed RNA samples from TG (NKCC1), spinal cord (KCC2) or kidney (NKCC2) and subsequently subcloned

into pGEM T-easy vector (Promega) and sequenced for verification. The subclones used to generate Dig-labeled cRNA probes were as follows: NKCC1 (AF051561) bps 872–1365, NKCC2 (U10096) bps 2281–2723 and KCC2 (U55816) bps 258–679. Dig-labeled riboprobes were synthesized from the linearized fragment-containing constructs using The Riboprobe Combination System SP6/T7 (Promega) incorporating 1 mM ATP, CTP and GTP with 650 μ M unlabeled UTP and 350 μ M Dig-labeled UTP (Roche, Indianapolis, IN). Riboprobes were purified by G-50 column chromatography (Roche) and stored in hybridization buffer containing 50% formamide, 0.3 M NaCl, 10 mM Tris, 1 mM EDTA, 1 \times Denhardt's solution, 10% dextran sulfate and 50 μ g/ml yeast tRNA (Roche).

Tissue sections were prepared for hybridization by fixing in ice-cold 3.7% formaldehyde for 1 h and permeabilizing with 0.5% Triton X-100 in 0.1 M Tris/0.05 M EDTA for 30 min. Sections were then acetylated with acetic anhydride for 10 min, dehydrated, delipidated with chloroform and rehydrated. Sections were then hybridized in a humidified chamber with riboprobes (100 ng/ml) in hybridization buffer for 16 h at 55 $^{\circ}$ C. Following hybridization, sections were washed with 4 \times SSC 4 times and treated with RNase I (20 μ g/ml, Roche) for 30 min at 37 $^{\circ}$ C. Washes were performed in decreasing concentrations of SSC, culminating in a final high stringency wash in 0.1 \times SSC at 55 $^{\circ}$ C for 30 min, then dehydrated and allowed to air dry. Slides were then blocked for 30 min in normal goat serum (NGS) and exposed to sheep anti-Dig-Fab fragments (Roche) for 1 h. Following washing, the alkaline phosphatase reaction was developed with BCIP/NBT solution (Roche) for 18 h.

4.5. Double labeling ISH/Immunohistochemistry (IHC)

All sections were first subjected to ISH as described above; however, following the development of the hybridization, signal sections were blocked in PBS containing 10% normal goat serum (NGS, Wisent, Montreal, QC) 3 times for 10 min. Next, primary antibody directed against CGRP (Sigma; rabbit polyclonal 1:1000), TRPV1 (Guo et al., 1999; Neuromics; guinea pig (C-terminal) and rabbit (N-terminal) polyclonal 1:2000), neurofilament 200 (Parysek and Goldman, 1988; N52, Sigma; mouse monoclonal 1:600), calcium-calmodulin kinase II α (CaMKII α , Chemicon, mouse monoclonal 1:1000) or peripherin (Goldstein et al., 1991; Sigma; rabbit polyclonal 1:1000) diluted in PBS containing 10% NGS and 0.1% sodium azide were then applied and incubated overnight at 4 $^{\circ}$ C. Sections were then washed 3 times in PBS and incubated for 1 h at room temperature in the appropriate secondary antibody (goat anti-rabbit, anti-guinea pig or anti-mouse diluted at 1:600) conjugated to Alexa-Fluor 488 or 568 (Molecular Probes, Eugene, OR). Slides were then coverslipped with BioMeda mounting media (Biomedica) and allowed to dry.

4.6. IHC for NKCC1 combined with TRPV1, N52 or NG2

Slide mounted sections were fixed in ice-cold 3.7% paraformaldehyde in 1 \times PBS for 1 h and then washed 3 \times 5 min in PBS. Slides were then transferred to 0.1 M sodium citrate, 0.05% Tween-20 solution and microwaved on 100% power for 1.5 min followed by 8.5 min on 20% power in a 900-Watt microwave

oven for antigen retrieval. After 30 min cool down, slides were again transferred to 1 \times PBS and washed 3 \times 5 min and then permeabilized in 1 \times PBS containing 0.05% Triton X-100. Slides were then blocked for at least 1 h in 1 \times PBS, 10% NGS solution prior to addition of antibodies. The NKCC1 rabbit polyclonal, affinity-purified antibodies used (kindly provided by Dr. Christian Lytle, University of California at Riverside) were antibody NT (characterized in McDaniel et al., 2005; Wang et al., 2003), directed against the entire cytoplasmic N-terminus of human NKCC1, and antibody TEFS-2 (characterized in Del Castillo et al., 2005), directed against the entire cytoplasmic C-terminus of human NKCC1. We have utilized the terminology NT and TEFS-2 to refer to these NKCC1 antibodies throughout the manuscript because these are the names given to these particular antibodies in the references where they are characterized, as listed above. The NT and TEFS-2 antibodies were used at a 1:200 dilution. The NKCC1 antibodies were incubated overnight at 4 $^{\circ}$ C and visualized with goat anti-rabbit Alexa-Fluor 488 or 568. Anti-TRPV1 (guinea pig polyclonal, Neuromics), neurofilament 200 (N52, mouse monoclonal, Sigma) or NG2 chondroitin-sulfate proteoglycan antigen (Levine and Card, 1987; Chemicon, mouse monoclonal, 1:200 dilution) antibodies were then incubated for an additional overnight period and visualized with goat anti-guinea pig Alexa-Fluor 568 or goat anti-mouse Alexa-Fluor 488 secondary antibodies.

4.7. Image acquisition and analysis

All ISH and ISH/IHC images were acquired using an Axioplan 2 imaging system (Zeiss) connected to an axiocam HRC camera (Zeiss). Images were analyzed using Axiovision 4.1 (Zeiss). Confocal IHC images were taken using an Axiovert 100 M confocal microscope (Zeiss). For ISH/IHC colocalization, neurons were assigned as either NKCC1-positive or NKCC1-negative based on the presence of signal above background. Background was standardized using sense orientation NKCC1 riboprobes processed alongside antisense oriented probe reactions that gave an average pixel value for background. From this value signal in antisense, ISH reactions could be determined as above or below background using Axioplan software. For the IHC portion of double labeling experiments, all neurons displaying fluorescent signal above background were counted as IHC-positive. This was defined by scaling the image, using Axiovision's built-in scaling feature, to an average pixel value for negative neurons and establishing all neurons as positive that were above that threshold. Colocalization was assessed by overlaying the corresponding double-labeled images and assessing the co-presence of NKCC1 mRNA with the immuno-analyte of interest. For each condition, 5 non-overlapping images from DRG and TG were taken and assessed for colocalization from 3 different animals. At least 500 neurons were assessed per animal. To measure neuronal size profiles, 40 \times images were acquired and positive neurons with visible nuclei were measured for total area. Neurons were outlined using Axiovision 4.1, and their area was determined using the built-in feature of the software. Total area was then converted to an average diameter, and these values were binned to create neuron size frequency profiles. Since stereological techniques were not used to measure

neuron diameters, the results presented may represent a biased estimate of the true distribution of diameters, hence, these data are referred to as profiles. Data are presented as mean \pm SEM for colocalization in both the DRG and TG.

Acknowledgments

This work was supported by grants from the Canadian Foundation for Innovation (CFI), the Canadian Institutes of Health Research (CIHR) and the Fonds de la Recherche en santé du Québec (FRSQ) to FC. TJP is a NIH NRSA Fellow (NS049772), FC is the holder of a CIHR Research Chair. The authors are grateful to Lisa Krawec for expert technical assistance and to Dr. Alfredo Ribiero-da-Silva and Jacynthe Laliberte for microscopy advice and equipment use.

REFERENCES

- Alvarez-Leefmans, F.J., Gamino, S.M., Giraldez, F., Noguero, I., 1988. Intracellular chloride regulation in amphibian dorsal root ganglion neurones studied with ion-selective microelectrodes. *J. Physiol.* 406, 225–246.
- Alvarez-Leefmans, F.J., Leon-Olea, M., Mendoza-Sotelo, J., Alvarez, F.J., Anton, B., Garduno, R., 2001. Immunolocalization of the Na (+)-K(+)-2Cl(-) cotransporter in peripheral nervous tissue of vertebrates. *Neuroscience* 104, 569–582.
- Balakrishnan, V., Becker, M., Lohrke, S., Nothwang, H.G., Guresir, E., Friauf, E., 2003. Expression and function of chloride transporters during development of inhibitory neurotransmission in the auditory brainstem. *J. Neurosci.* 23, 4134–4145.
- Caterina, M.J., Schumacher, M.A., Tominaga, M., Rosen, T.A., Levine, J.D., Julius, D., 1997. The capsaicin receptor: a heat-activated ion channel in the pain pathway. *Nature* 389, 816–824.
- Caterina, M.J., Leffler, A., Malmberg, A.B., Martin, W.J., Trafton, J., Petersen-Zeitz, K.R., Koltzenburg, M., Basbaum, A.I., Julius, D., 2000. Impaired nociception and pain sensation in mice lacking the capsaicin receptor. *Science* 288, 306–313.
- Cervero, F., Laird, J.M., 1996. Mechanisms of touch-evoked pain (allodynia): a new model. *Pain* 68, 13–23.
- Cervero, F., Laird, J.M., Garcia-Nicas, E., 2003. Secondary hyperalgesia and presynaptic inhibition: an update. *Eur. J. Pain* 7, 345–351.
- Coggeshall, R.E., Carlton, S.M., 1997. Receptor localization in the mammalian dorsal horn and primary afferent neurons. *Brain Res. Brain Res. Rev.* 24, 28–66.
- DeFazio, R.A., Keros, S., Quick, M.W., Hablitz, J.J., 2000. Potassium-coupled chloride cotransport controls intracellular chloride in rat neocortical pyramidal neurons. *J. Neurosci.* 20, 8069–8076.
- Del Castillo, I.C., Fedor-Chaiken, M., Song, J.C., Starlinger, V., Yoo, J., Matlin, K.S., Matthews, J.B., 2005. Dynamic regulation of Na (+)-K(+)-2Cl(-) cotransporter surface expression by PKC-[epsilon] in Cl(-)-secretory epithelia. *Am. J. Physiol.: Cell Physiol.* 289, C1332–C1342.
- Galan, A., Cervero, F., 2005. Painful stimuli induce in vivo phosphorylation and membrane mobilization of mouse spinal cord NKCC1 co-transporter. *Neuroscience* 133, 245–252.
- Garcia-Nicas, E., Laird, J.M., Cervero, F., 2006. GABA-A receptor blockade reverses the injury-induced sensitization of Nociceptor Specific (NS) neurons in the spinal dorsal horn of the rat. *J. Neurophysiol.* 96, 661–670.
- Goldstein, M.E., House, S.B., Gainer, H., 1991. NF-L and peripherin immunoreactivities define distinct classes of rat sensory ganglion cells. *J. Neurosci. Res.* 30, 92–104.
- Goldstein, M.E., Grant, P., House, S.B., Henken, D.B., Gainer, H., 1996. Developmental regulation of two distinct neuronal phenotypes in rat dorsal root ganglia. *Neuroscience* 71, 243–258.
- Granados-Soto, V., Arguelles, C.F., Alvarez-Leefmans, F.J., 2005. Peripheral and central antinociceptive action of Na⁺-K⁺-2Cl⁻ cotransporter blockers on formalin-induced nociception in rats. *Pain* 114, 231–238.
- Guo, A., Vulchanova, L., Wang, J., Li, X., Elde, R., 1999. Immunocytochemical localization of the vanilloid receptor 1 (VR1): relationship to neuropeptides, the P2X3 purinoceptor and IB4 binding sites. *Eur. J. Neurosci.* 11, 946–958.
- Hammond, D.L., Ackerman, L., Holdsworth, R., Elzey, B., 2004. Effects of spinal nerve ligation on immunohistochemically identified neurons in the L4 and L5 dorsal root ganglia of the rat. *J. Comp. Neurol.* 475, 575–589.
- Hanani, M., 2005. Satellite glial cells in sensory ganglia: from form to function. *Brain Res. Brain Res. Rev.* 48, 457–476.
- Kaila, K., Pasternack, M., Saarikoski, J., Voipio, J., 1989. Influence of GABA-gated bicarbonate conductance on potential, current and intracellular chloride in crayfish muscle fibres. *J. Physiol.* 416, 161–181.
- Kaila, K., Lamsa, K., Smirnov, S., Taira, T., Voipio, J., 1997. Long-lasting GABA-mediated depolarization evoked by high-frequency stimulation in pyramidal neurons of rat hippocampal slice is attributable to a network-driven, bicarbonate-dependent K⁺ transient. *J. Neurosci.* 17, 7662–7672.
- Kanaka, C., Ohno, K., Okabe, A., Kuriyama, K., Itoh, T., Fukuda, A., Sato, K., 2001. The differential expression patterns of messenger RNAs encoding K-Cl cotransporters (KCC1,2) and Na-K-2Cl cotransporter (NKCC1) in the rat nervous system. *Neuroscience* 104, 933–946.
- Kaneko, H., Putzier, I., Frings, S., Kaupp, U.B., Gensch, T., 2004. Chloride accumulation in mammalian olfactory sensory neurons. *J. Neurosci.* 24, 7931–7938.
- Laird, J.M., Garcia-Nicas, E., Delpire, E.J., Cervero, F., 2004. Presynaptic inhibition and spinal pain processing in mice: a possible role of the NKCC1 cation-chloride co-transporter in hyperalgesia. *Neurosci. Lett.* 361, 200–203.
- Lawson, S.N., McCarthy, P.W., Prabhakar, E., 1996. Electrophysiological properties of neurones with CGRP-like immunoreactivity in rat dorsal root ganglia. *J. Comp. Neurol.* 365, 355–366.
- Levine, J.M., Card, J.P., 1987. Light and electron microscopic localization of a cell surface antigen (NG2) in the rat cerebellum: association with smooth protoplasmic astrocytes. *J. Neurosci.* 7, 2711–2720.
- Lytle, C., Xu, J.C., Biemesderfer, D., Forbush 3rd, B., 1995. Distribution and diversity of Na-K-Cl cotransport proteins: a study with monoclonal antibodies. *Am. J. Physiol.* 269, C1496–C1505.
- McDaniel, N., Pace, A.J., Spiegel, S., Engelhardt, R., Koller, B.H., Seidler, U., Lytle, C., 2005. Role of Na-K-2Cl cotransporter-1 in gastric secretion of nonacidic fluid and pepsinogen. *Am. J. Physiol.: Gastrointest. Liver Physiol.* 289, G550–G560.
- Mikawa, S., Wang, C., Shu, F., Wang, T., Fukuda, A., Sato, K., 2002. Developmental changes in KCC1, KCC2 and NKCC1 mRNAs in the rat cerebellum. *Brain Res. Dev. Brain Res.* 136, 93–100.
- Nickell, W.T., Kleene, N.K., Gesteland, R.C., Kleene, S.J., 2005. Neuronal chloride accumulation in olfactory epithelium of mice lacking NKCC1. *J. Neurophysiol.* 95, 2003–2006.
- Parysek, L.M., Goldman, R.D., 1988. Distribution of a novel 57 kDa intermediate filament (IF) protein in the nervous system. *J. Neurosci.* 8, 555–563.

- Parysek, L.M., Chisholm, R.L., Ley, C.A., Goldman, R.D., 1988. A type III intermediate filament gene is expressed in mature neurons. *Neuron* 1, 395–401.
- Payne, J.A., Rivera, C., Voipio, J., Kaila, K., 2003. Cation–chloride co-transporters in neuronal communication, development and trauma. *Trends Neurosci.* 26, 199–206.
- Plotkin, M.D., Kaplan, M.R., Peterson, L.N., Gullans, S.R., Hebert, S. C., Delpire, E., 1997. Expression of the Na(+)-K(+)-2Cl-cotransporter BSC2 in the nervous system. *Am. J. Physiol.* 272, C173–C183.
- Price, T.J., Cervero, F., de Koninck, Y., 2005. Role of cation–chloride-cotransporters (CCC) in pain and hyperalgesia. *Curr. Top. Med. Chem.* 5, 547–555.
- Reisert, J., Lai, J., Yau, K.W., Bradley, J., 2005. Mechanism of the excitatory Cl(–) response in mouse olfactory receptor neurons. *Neuron* 45, 553–561.
- Rezajooi, K., Pavlides, M., Winterbottom, J., Stallcup, W.B., Hamlyn, P.J., Lieberman, A.R., Anderson, P.N., 2004. NG2 proteoglycan expression in the peripheral nervous system: upregulation following injury and comparison with CNS lesions. *Mol. Cell. Neurosci.* 25, 572–584.
- Rivera, C., Voipio, J., Kaila, K., 2005. Two developmental switches in GABAergic signalling: the K+–Cl–cotransporter KCC2 and carbonic anhydrase CAVII. *J. Physiol.* 562, 27–36.
- Rudomin, P., Schmidt, R.F., 1999. Presynaptic inhibition in the vertebrate spinal cord revisited. *Exp. Brain Res.* 129, 1–37.
- Schmidt, R.F., 1971. Presynaptic inhibition in the vertebrate central nervous system. *Ergeb. Physiol.* 63, 20–101.
- Schomberg, S.L., Su, G., Haworth, R.A., Sun, D., 2001. Stimulation of Na–K–2Cl cotransporter in neurons by activation of Non-NMDA ionotropic receptor and group-I mGluRs. *J. Neurophysiol.* 85, 2563–2575.
- Staley, K.J., Soldo, B.L., Proctor, W.R., 1995. Ionic mechanisms of neuronal excitation by inhibitory GABAA receptors. *Science* 269, 977–981.
- Sung, K.W., Kirby, M., McDonald, M.P., Lovinger, D.M., Delpire, E., 2000. Abnormal GABAA receptor-mediated currents in dorsal root ganglion neurons isolated from Na–K–2Cl cotransporter null mice. *J. Neurosci.* 20, 7531–7538.
- Svenningsen, A., Colman, D., Pedraza, L., 2004. Satellite cells of dorsal root ganglia are multipotential glial precursors. *Neuron Glia Biol.* 1, 85–93.
- Szabadics, J., Varga, C., Molnar, G., Olah, S., Barzo, P., Tamas, G., 2006. Excitatory effect of GABAergic axo-axonic cells in cortical microcircuits. *Science* 311(2006), 233–235.
- Toyoda, H., Yamada, J., Ueno, S., Okabe, A., Kato, H., Sato, K., Hashimoto, K., Fukuda, A., 2005. Differential functional expression of cation–Cl(–) cotransporter mRNAs (KCC1, KCC2, and NKCC1) in rat trigeminal nervous system. *Brain Res. Mol. Brain Res.* 133, 12–18.
- Wang, H., Yan, Y., Kintner, D.B., Lytle, C., Sun, D., 2003. GABA-mediated trophic effect on oligodendrocytes requires Na–K–2Cl cotransport activity. *J. Neurophysiol.* 90, 1257–1265.
- Willis Jr., W.D., 1999. Dorsal root potentials and dorsal root reflexes: a double-edged sword. *Exp. Brain Res.* 124, 395–421.
- Zhu, L., Lovinger, D., Delpire, E., 2005. Cortical neurons lacking KCC2 expression show impaired regulation of intracellular chloride. *J. Neurophysiol.* 93, 1557–1568.